Efficient Parathyroidectomy Guided by SPECT-MIBI and Hormonal Measurements

G.N. Sfakianakis, G.L. Irvin III, J. Foss, W. Mallin, M. Georgiou, G.T. Deriso, A.S. Molinari, S. Ezuddin, W. Ganz, A. Serafini, A.M. Jabir and S.K.C. Chandarlapaty

Division of Nuclear Medicine, Departments of Radiology and Surgery, University of Miami School of Medicine, Jackson Memorial Hospital; and Veterans Affairs Medical Center, Miami, Florida

Parathyroidectomy is a difficult and lengthy operation which is noncurative in 6% to 10% of cases. To improve the efficiency of this operation, a new dual diagnostic approach was prospectively applied. **Methods:** Preoperative tomographic ^{99m}Tc-sestamibi (MIBI) scintigraphy and intraoperative measurements of circulating parathyroid hormone (PTH) levels by a quick assay (QPTH) were used. Scintigraphy comprised immediate and delayed planar and SPECT of the neck and chest, following 20 mCi MIBI. The presence and location of persistent foci of abnormal activity found within the neck and mediastinum on volume-rendered reprojection (RPJ) of the SPECT data were reported. The surgeon, guided by the three-dimensional MIBI-SPECT/RPJ images, identified and excised the single or most prominent scintigraphic focus and applied the QPTH. If PTH levels fell from baseline by at least 50%, the operation was concluded. **Results:** The operative time of primary parathyroidectomy was reduced from an average of 90 min (before the introduction of scintigraphy and intraoperative PTH measurements) to 57 min. All but two patients became normocalcemic. In 58 consecutive patients with hyperparathyroidism, MIBI-SPECT/RPJ correctly and precisely identified 51 of 53 (96%) primary parathyroid adenomas, 14 of 15 secondary hyperplasias and 2 of 3 hyperplastic glands in MEN (sensitivity 94%, specificity 92%). QPTH verified the excision of the primary parathyroid adenomas and predicted normocalcemia in 50 of 52 patients. In 6 patients with misleading scintigraphy, QPTH was especially useful and guided the surgeon to continue the operation until the abnormal parathyroid tissue was found and excised. **Conclusion:** MIBI-SPECT/RPJ and QPTH sequentially applied improved the efficiency of parathyroidectomy.

Key Words: parathyroidectomy; hyperparathyroidism; ^{99m}Tc-MIBI/SPECT; parathyroid hormone measurements

J Nucl Med 1996; 37:798-804

Parathyroidectomy is a difficult and lengthy operation which fails to cure a significant number of patients. Preoperative imaging of the abnormal parathyroid gland(s) is helpful and widely practiced. Scintigraphic methods of localization of parathyroid gland pathology have been found by several investigators to be more useful than other imaging modalities (*1–12*). The introduction of the isonitrile compound ^{99m}Tc-sestamibi (MIBI) (*13*) increased the sensitivity of scintigraphy to 90% (*14,15*). MIBI was originally used with ^{123}INa and subtraction techniques (*14*), but because abnormal parathyroid glands retain MIBI much longer than thyroid tissue, subtraction techniques proved to be unnecessary and early and late MIBI imaging was introduced (*15*). MIBI imaging has been performed in planar mode and, despite improved sensitivity, false negative studies have been reported. In addition, although the new methodology indicated the axial and the lateral distance of the lesions from the thyroid gland, which served as an anatomic landmark, it could not provide information regarding depth from the anterior surface. More recent observations have confirmed the high sensitivity of MIBI studies, but emphasize the fact that MRI is needed for in-depth localization (*16*).

Parathyroidectomy has not been curative in 6–8% of cases. Previous work performed at our institution indicated that the efficiency of parathyroidectomy was greatly improved when a successful excision of a targeted lesion was verified by intraoperative monitoring of parathyroid hormone (PTH) blood levels (*17–21*). A quick PTH assay (QPTH) was used. Because the half life of the intact hormone in the blood is 3–4 min, a marked decrease in PTH level after excision of a single large adenoma predicts operative success with return to normocalcemia. Conversely, persistent high levels of PTH point to excess secretion by residual gland(s), indicating the need for further exploration.

This study evaluated the effect on the duration and results of parathyroidectomy of a combined application of preoperative three-dimensional localization and intraoperative verification of excision of all hyperfunctioning parathyroid tissue. We report the results of a 2-yr application of MIBI/SPECT studies for preoperative three-dimensional localization of parathyroid pathology and intraoperative measurements of peripheral PTH by QPTH. Preliminary and interim observations were presented in surgical and nuclear medicine meetings (*22,23*).

MATERIALS AND METHODS

Patients

Sixty-two consecutive patients (3:1, female:male) with the established diagnosis of hyperparathyroidism (elevated preoperative serum calcium levels and intact parathyroid hormone levels above the normal range for the individual assays used) were studied with MIBI scintigraphy. Of these, three patients with only planar studies and one patient with inconclusive surgical data were excluded. A total of 58 patients, 52 with primary hyperparathyroidism (one found to have two adenomas), 4 with secondary (hyperplasia of all glands) and 2 with MEN (with one and two hyperfunctioning glands), had MIBI-SPECT studies. Five patients had undergone previous neck explorations for thyroid or parathyroid disease. All primary patients had normal serum creatinine values except one (2.1 mg/dl) who had a late recurrence of hypercalcemia 10 yr after his first parathyroidectomy.

Scintigraphy

As part of the preoperative evaluation, ^{99m}Tc-sestamibi (Cardiolite, DuPont Merck Pharmaceutical Co., Billerica, MA) parathyroid gland scintigraphy was performed. Doses of 20 mCi (7400 MBq) were injected intravenously and patients were studied immediately after injection by both planar and SPECT imaging using a Trionix (Twinsburg, OH) three-detector camera. Patients were reexamined between 2–5½ hr after the injection, depending on the daily

Received Mar. 24, 1995; revision accepted Sept. 7, 1995.

For correspondence or reprints contact: George N. Sfakianakis, MD, Division of Nuclear Medicine (D-57), University of Miami School of Medicine, P.O. Box 016960, Miami, FL 33101.

schedule and camera availability. Planar images preceded SPECT during both early and late imaging sessions.

For planar imaging, a 500 thousand-count image of the neck and chest was obtained in anterior projection with a parallel-hole, low-energy, ultrafine resolution collimator for an imaging time of 5–10 min. Standard protocols were used for SPECT acquisition, processing and reprojection. Briefly, the SPECT studies were acquired in 64 × 64 × 16 bits/pixel matrix size with a low-energy ultrafine resolution collimator, in step and shoot rotation type of 4° per step, in a noncircular orbit, for 40 sec per projection. A slice-smoothing A (z axis) filter with kernel of size 5: [1 2 5 2 1] and a Hamming filter with 1.10 cyc/cm high cutoff frequency (Nyquist 1.404 cyc/cm) were used for reconstruction. The reprojection (RPJ) algorithm applied to the reconstructed volume of SPECT data generates 36 sequential images, 128 × 128 × 16 bits/pixel, which simulate the perspective of this volume as a spectator from the outside would see it; these images (SPECT/RPJ) are angled 10° apart and cover the entire 360° circumference of the reconstructed volume of the data. When projected sequentially fast enough, they provide the standard volume-rendered display (*24*). This display helps the observer to better appreciate the lesions and ignore the noise.

Planar images were interpreted on a computer display monitor. The reprojected tomographic data was reviewed and interpreted using both a cinematic display (volume display) and a static review of the individual 36 views. Selected individual views from the cinematic reprojection data have been provided for this publication (anterior, left or right 45° oblique, and left or right lateral views).

Two nuclear medicine physicians, with knowledge of the clinical history, followed a predetermined set of criteria to review all the SPECT/RPJ studies retrospectively in conference and without the planar images. Planar images were reviewed independently and without knowledge of the tomographic findings; the results of the planar studies were used only for comparison with the SPECT/RPJ studies. Finally, scintigraphic data, as presented in this paper, are based on the retrospective review and differ slightly from the original interpretations, which the surgeon had available at the time of the operation.

The scintigraphic criteria set forth as indicative of potential parathyroid lesion(s) were the following:

1. Focal sestamibi accumulation(s) present in both the immediate and the delayed images (which conventionally qualify as hyperfunctioning parathyroid glands). Lesions covered by the thyroid gland in the early images but identifiable in delayed views were also considered to be parathyroid lesions.
2. Foci located only in the neck below the salivary glands or in the mediastinum above the heart.

The cervical foci were subdivided into left or right, superior, middle and inferior in relation to the lateral lobe of the thyroid gland. Mediastinal foci were subdivided into superior (often found in the vicinity of the thymus gland) and middle/inferior (below the aortic arch and not accessible from the neck for resection). The depth of the focus in the neck was also related to the thyroid gland, and foci were characterized as anterior (within the thyroid) (Fig. 1), juxtathyroidal (adjacent to the lateral margin of the thyroid) and posterior (posterior to the thyroid) (Fig. 2). If multiple foci were found, these were classified in numerical order beginning with the most intense focus (focus no. 1) and continuing in order of decreasing intensity/size (focus no. 2, etc.) (Fig. 3). Additional scintigraphy was used for better localization of mediastinal lesions (skeletal and blood pool, Fig. 4), or for differentiation of parathyroid adenomas from lymphomas (^{67}Ga, Fig. 5).

The population studied was highly selective and included only patients with clinical and laboratory proof of hyperparathyroidism.

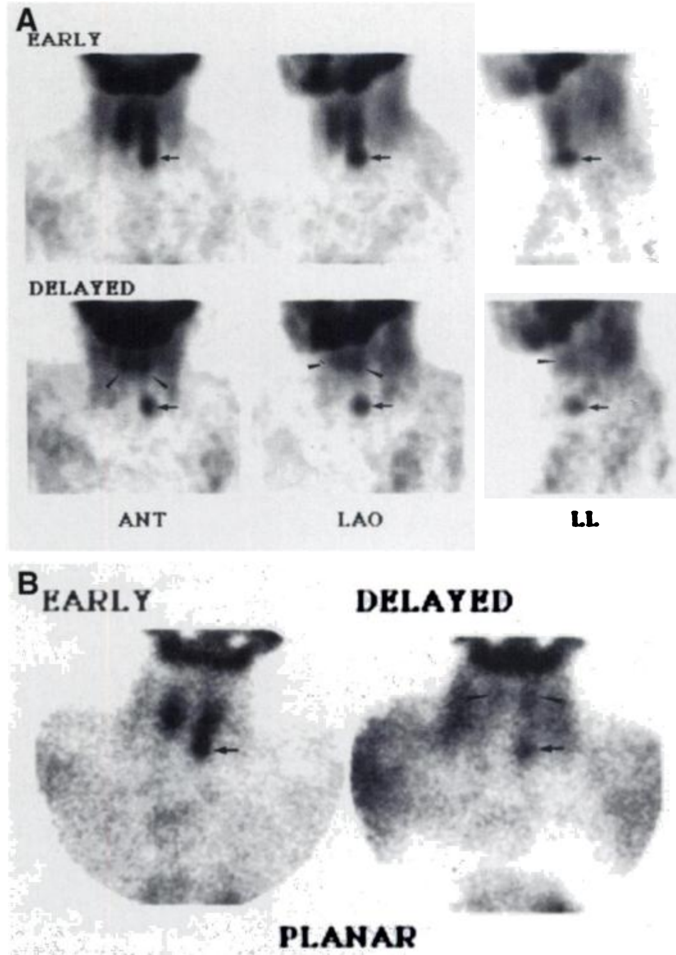

FIGURE 1. (A) Selected MIBI-SPECT/RPJ images illustrating a primary parathyroid adenoma in left lower cervical position anteriorly (arrows). In the lateral view (LL) the lesion appears in the same plane with the thyroid gland. On the delayed images a butterfly-like midline activity (arrow heads) is perceived, probably strap muscle activity. (B) Planar images of case shown in A.

No controls were used. Therefore, the normal parathyroid glands found surgically or expected to be present in these patients were considered as true negatives for the calculation of specificity. Standard methods were used for calculation of sensitivity, positive and negative predicted value of scintigraphy. SPECT results were compared to planar using the chi square test.

Quick PTH Assay

The intact parathyroid hormone was measured in most patients by an intraoperative quick intact PTH assay (QPTH) which has been reported previously (*21*). This immunochemiluminometric assay (Nichols Institute Diagnostics, San Juan Capistrano, CA) was found to correlate well ($r = 0.9218$, $p < 0.0001$) with the standard 24-hr immunoradiometric assay (*21*). Briefly, peripheral blood was used and plasma from a 15-sec microcentrifugation was mixed with two antibodies, incubated at 45°C, shaken at 400 rpm for 7 min, washed and counted for 2 sec on a portable luminometer, allowing the PTH level to be reported in 10 min (*21*). PTH levels were measured 5 min after excision of a suspected abnormal gland and compared with preoperative or pre-excision samples. A fall of at least 50% in PTH levels was considered confirmation of complete excision of all abnormal parathyroid tissue. The sensitivity of this test in predicting postoperative calcium levels has been reported as 94% (*21*).

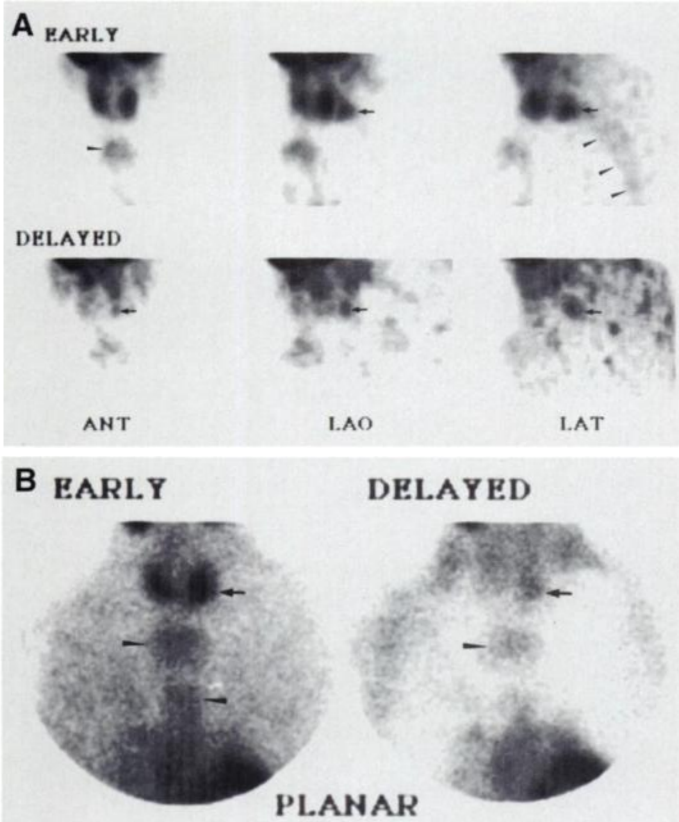

FIGURE 2. (A) Selected MIBI-SPECT/RPJ images illustrating a parathyroid adenoma in the left lower cervical position posteriorly (arrows). In the lateral view the adenoma is clearly visible adjacent to the faint image of the bone marrow of the vertebral column (arrow heads). Bone marrow activity is also present in the manubrium sterni (arrow head). At surgery the adenoma was found at the level of the esophagus. The SPECT/RPJ images were especially useful in guiding the surgeon to select the depth of exploration and persistently search for the lesion. (B) Planar images of case shown in A. On the delayed image, the lesion is barely visible as compared to the clear and in-depth visualization on the SPECT/RPJ (A). Bone marrow activity of the sternum is prominent on the early and, less evident, on the delayed images (arrow heads).

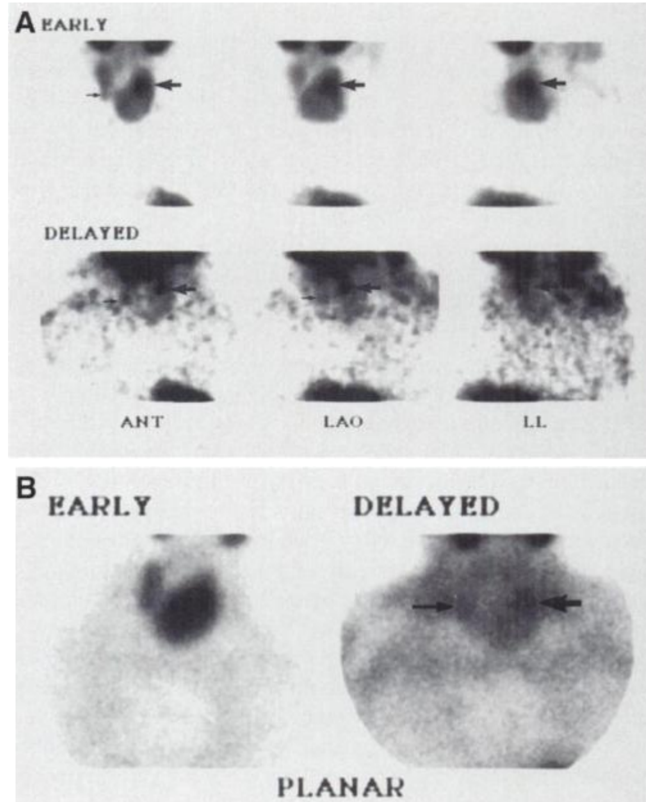

FIGURE 3. (A) Selected MIBI-SPECT/RPJ images from a study of a patient who had a goiter and hyperparathyroidism. Two abnormal cervical foci were identified, one on the left (large arrow) and one on the right (small arrow). In this case the dominant focus (no. 1) was first excised, but the PTH did not fall and frozen biopsy showed that it was of thyroid origin. The surgeon then resected the second focus (no. 2) which proved to be the parathyroid adenoma. When this was removed, the PTH fell to less than 50%. (B) Planar images of the case shown in A. The two foci could be recognized only retrospectively on the delayed images.

Surgical Strategies

Surgical procedure was based on the scintigraphically identified exact location of each parathyroid abnormality as revealed three-dimensionally by MIBI-SPECT/RPJ. Exploration was directed to the involved site (the single focus or focus no. 1 of MIBI-SPECT/RPJ) and any grossly abnormal parathyroid gland was removed and sent to pathology for histological confirmation. Five minutes after the excision, a peripheral blood sample for QPTH was drawn for comparison with the pre-exploration sample. At this point, no further dissection was done and the wound was closed. The patient was kept under light anesthesia until the results of the QPTH assay were available. If the hormone level dropped by more than 50% in the 5-min post-excision sample, the patient was awakened and returned to the recovery room. However, if the primary lesion was not identified or there was little or no decrease in the QPTH level after the primary lesion was excised, the closed wound was quickly opened and exploration continued for any remaining hyperfunctioning glands (no. 2 lesion, etc.). In the presence of high QPTH, surgical exploration was continued when the MIBI-SPECT/RPJ showed multiple lesions, was questionable, or was negative (2 cases with primary disease) until a large gland was excised and QPTH levels fell 50%. In all patients, the excised abnormal tissue was sent for pathological evaluation.

RESULTS

Surgical Results

Fifty-six of the 58 patients included in this analysis (52 with primary, 4 with secondary and 2 with MEN hyperparathyroidism) were cured by cervical parathyroidectomy as proven by postoperative normocalcemia. Two patients had each a middle/inferior mediastinal ectopic lesion by scintigraphy; each was noncured by cervical exploration and refused thoractomy. With the combined diagnostic approach of the MIBI-SPECT/RPJ and QPTH, the average operative time in the 52 patients with primary hyperparathyroidism was 57 min (range between 20–130 min). This was shorter than the time recorded for the same surgeon (90 min), when he operated without the help of scintigraphy or hormonal measurements in previous years.

The Role of Scintigraphy

The 58 patients had a total of 71 abnormal parathyroid glands excised and documented by pathology, except for the two inaccessible mediastinal ectopic glands. MIBI-SPECT/RPJ correctly visualized 67 of 71 abnormal glands with an overall sensitivity of 94%. There were 12 false-positive scintigraphic foci indicating a specificity of 92% (Table 1). For the primary lesions, the sensitivity and specificity of SPECT were slightly higher than for the entire population, 96% and 94%, respectively. Specificity was highest (98%) when the single or the most intense scintigraphic focus was considered diagnostic of parathyroid pathology, but this was at the expense of sensitivity (92%).

As shown in Table 2, topographically, the 71 abnormal

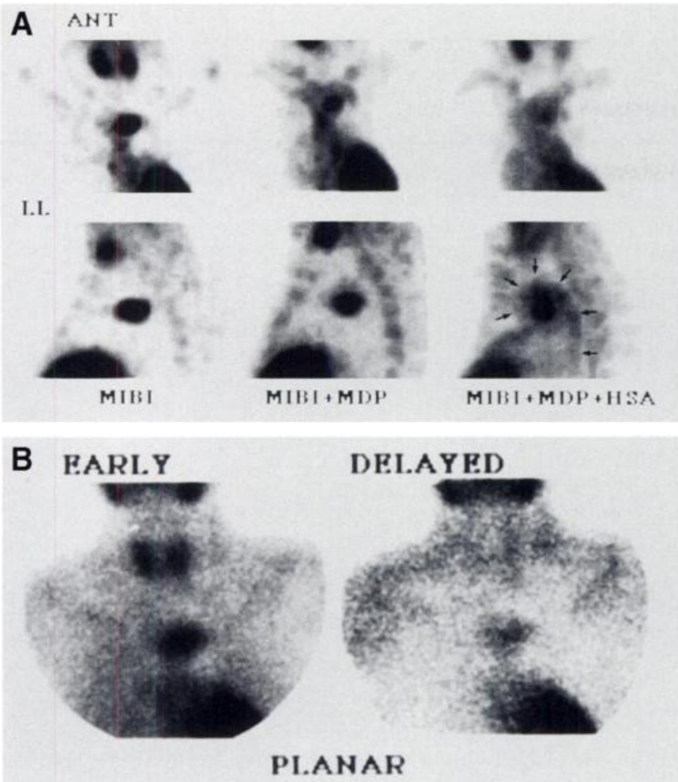

FIGURE 4. (A) A middle/lower mediastinal lesion is shown to be located below the aortic arch by combined MIBI, bone and blood pool imaging (SPECT/RPJ). The MIBI study was first performed and visualized a single lesion in the center of the chest (left images, MIBI). An attempt was made to excise the lesion from the neck but it was not accessible; right hemithyroidectomy with two-gland parathyroidectomy was performed when three normally appearing parathyroids but no adenoma were found in the neck. PTH levels did not decrease and the patient remained hypercalcemic. On reevaluation, MDP was injected overnight and 1 hr after MIBI injection imaging was performed (middle images, MIBI + MDP). Subsequently, HSA was injected and one more SPECT was acquired (right images, MIBI + MDP + HSA). The addition of MDP and HSA showed the lesion to be located below the aortic arch (small arrows). The patient refused thoracotomy. (B) Planar images from the first evaluation of the patient in A show the mediastinal lesion, but without information about its depth.

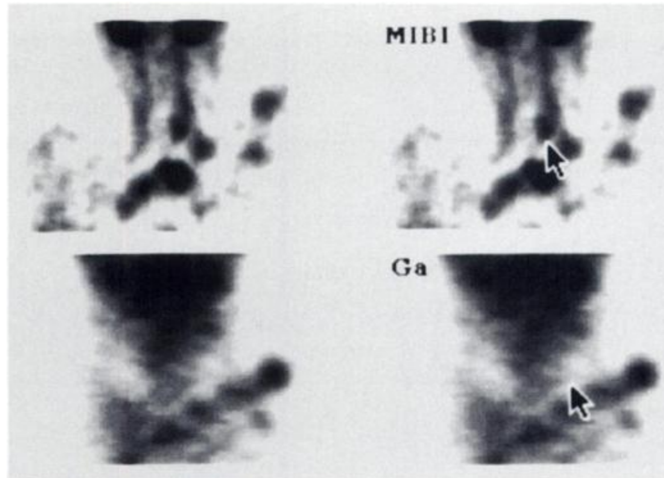

FIGURE 5. Selected anterior SPECT/RPJ images from MIBI and ^{67}Ga studies of a patient with known lymphoma who was also found to have hyperparathyroidism. The MIBI study revealed many abnormal foci in the neck of the patient. The ^{67}Ga study was performed to show which of these were lymphomas, expected to be visualized by ^{67}Ga; the one not visualized by ^{67}Ga (arrow) was the parathyroid adenoma, promptly found and excised; the operation lasted 25 min and the patient became normocalcemic.

glands were mostly cervical (only 4 mediastinal) and distributed equally on both sides. Most of the abnormalities were associated with the lower pole of the lateral lobes of the thyroid gland. Of the four patients with mediastinal abnormalities, two with superior mediastinal location were successfully operated and cured. Two patients with a middle/lower mediastinal lesion had cervical exploration but this approach failed as the lesion was below the aorta (Fig. 4).

The diagnostic significance of the single abnormal focus and of the relative intensity of the multiple abnormal foci is indicated in Table 3. A single focus, usually prominent and clearly visible, was present in a total of 45 studies and correctly identified in 44 an abnormal parathyroid gland. When multiple foci were present, the primary focus (no. 1) was also most frequently correct. The secondary focus (no. 2) was less often correct.

Interestingly, only one out of 52 patients with primary disease had a second abnormal gland. Scintigraphy visualized only one of them. Besides primary hyperparathyroidism, scintigraphic studies were successful in secondary and MEN disease. MIBI-SPECT/RPJ correctly identified 14 of 15 hyperplastic glands in 4 patients with secondary hyperparathyroidism. In one study a false-positive focus was present. In two patients with MEN, MIBI-SPECT/RPJ visualized one of the two adenomas in one patient and the single adenoma in the other. In the latter, two false-positive abnormal foci were present.

The four false-negative SPECT/RPJ studies (two among the primary, one in secondary and one in MEN) were further evaluated. One primary patient presented with a multinodular pattern of thyroidal activity, which was retained on the delayed images, and the abnormal parathyroid gland was invisible. In addition, this study was also false positive because it visualized a lymph node. The other primary patient had two abnormal parathyroid glands, one of which was visualized on both the early and delayed images, whereas the second was visible on the early studies alone. Interestingly, false-negative studies were not associated with the smallest abnormal parathyroid glands. Indeed, the size of the abnormal glands visualized by scintigraphy ranged between 0.7 × 0.78 × 0.4 cm (cervical left inferior) and 7.0 × 4.0 × 1.7 cm (cervical right inferior), and the false-negative glands had sizes 1.5 × 0.9 × 0.6 cm and 3.9 × 2.0 × 1.2 cm, respectively. In addition, it was noted that although the delayed images of the two false-negative studies were acquired after 3½ and 4 hr from injection time, respectively, in another 21 cases imaging was performed equally late and the abnormal glands were visible. As in cases of patients with primary hyperthyroidism, false-negative abnormal parathyroid glands in patients with secondary hyperplasias or MEN were not smaller but were also associated with delayed studies acquired at 3½ and 5½ hr. Previous partial thyroidectomy and exceptionally prominent muscles were factors potentially contributing to the nonrecognition of these two abnormal glands. In addition, some hyperplastic parathyroid glands were so prominently visible in the scans that others, less intense, were not seen initially.

None of the normal parathyroid glands was visualized. However, there were abnormal structures of other than parathyroid gland origin which were visualized and were ultimately responsible for the false-positive scintigraphic findings. Multiple lymphomatous lesions were visualized in a patient with non-Hodgkins lymphoma (Fig. 5). Among the 45 single foci of abnormal activity, there was one false-positive focus, which was identified as a hyperplastic lymph node. There were two false positive among the 13 high intensity (no. 1) abnormal foci in the cases with multiple scintigraphic lesions and they were

TABLE 1
Findings on MIBI-SPECT/RPJ Studies and Statistical Analysis of the Results in the Entire Population and in Each Group Studies

	Entire population	Primary hyperparathyroidism	Secondary hyperparathyroidism	Multi-endocrine neoplasia
Findings on MIBI-SPECT/RPJ				
True positive (abnormal parathyroids visualized)	67*	51 (49)†	14	2
True negative (normal parathyroids not visualized)	144	141	—	3
False positive (foci of activity of nonparathyroid origin)	12‡	9 (3)	1	2
False negative (abnormal parathyroids missed)	4	2 (4)	1	1
Statistical Analysis				
Sensitivity	94%	96% (92%)	—	—
Specificity	92%	94% (98%)	—	—
Positive predictive value	85%	85% (94%)	—	—
Negative predictive value	97%	99% (98%)	—	—

*The numbers indicate data for all abnormal foci of activity found on the SPECT/RPJ studies.
†Inside parenthesis are data when the single or the most intense focus of abnormal activity per patient/study was considered indicative of parathyroid pathology.
‡ Lymphomatous lesions present in one study were not included (Fig. 5).

identified as a thyroid adenoma in one patient (Fig. 3), and as a lymph node and Hashimoto's thyroiditis in the other. Among the less intense abnormal foci there were 9 false positive (7 of 13 no. 2, 1 of 5 no. 3 and 1 of 3 no. 4 in decreasing sequence of intensity/size). Two thyroid nodules and a lymph node were identified at surgery to account for 3 of them. The identity of 6 other false-positive foci remained unknown because QPTH fell and the operation was concluded without their exploration.

The normal thyroid gland was visible on the early images in most patients (Fig. 1–4). Thyroidectomy or thyroxine suppression were the cause of nonvisualization of this gland in a few patients. In all but two cases, the thyroid image was markedly reduced in intensity or disappeared by 2–5 hr. In 2 patients, the gland was visualized equally well on the delayed studies. This was believed to be due to thyroiditis. Finally, in 4 patients benign thyroid lesions retained the radioactivity as dominant (no. 1) (Fig. 3), or less intense (no. 2) foci.

The salivary glands were the most prominent organs in the neck, particularly on the delayed images. As such, brightness and contrast adjustment on the display monitor were frequently needed to visualize the less prominent parathyroid lesions on delayed images.

The bone marrow (Figs. 2,4) and some groups of muscles (Fig. 1) were faintly visible, especially on the delayed images. Symmetric butterfly-like activity, most probably of muscular origin, was nearly always present above the thyroid gland on delayed images (Fig. 1).

Finally, a blind reading of the planar studies was performed by the same with SPECT interpreters during different sessions and with the same clinical information. Planar images failed to visualize 8 abnormal parathyroid glands, as compared to only 4 missed by SPECT/RPJ; conversely, planar images visualized 8 false-positive foci, as compared to 9 of the SPECT/RPJ. This gave planar imaging a sensitivity of 84% and a specificity of 95%, not statistically different from SPECT/RPJ ($p < 0.1$). Of course, planar images did not provide information about the depths of the lesions. The surgeon, however, operated with full knowledge of the three-dimensional results and after a thorough review of the SPECT/RPJ volume and individual images. Therefore, the effect of planar studies on the success and duration of parathyroidectomy could not be assessed in this population.

Role of QPTH Measurements

Intraoperative QPTH measurements were performed in the 52 patients with primary hyperparathyriodism. In all the test was useful and correctly predicted the results of the operation, normocalcemia in 50 and persistent hypercalcemia in 2. More specifically, in 44 of these patients including the patient with lymphoma, the intraoperative QPTH measurements confirmed the excision of all abnormal tissue after a single true-positive

TABLE 2
Topographic Distribution of the Persistent Abnormal Foci of Increased Activity Found on MIBI-SPECT/RPJ Studies

	Right cervical			Left cervical			Mediastinal	
	True positive	False negative	False positive	True positive	False negative	False positive	True positive	False positive
Superior	5 (2)*	1 (0)	2 (2)	6 (3)	—	5 (4)	2 (2)	1 (0)
Middle	4 (4)	—	1 (0)	5 (4)	1 (0)	1 (1)	2 (2)	—
Inferior	24 (19)	2 (2)	1 (1)	19 (15)	—	1 (1)	—	—
Total	33 (25)	3 (2)	4 (3)	30 (22)	1 (0)	7 (6)	4 (4)	1 (0)

*The numbers outside parenthesis are data from the entire population; inside parenthesis are data from patients with primary hyperparathyroidism.

TABLE 3
Diagnostic Significance of the Single Scintigraphic Focus and of the Relative Size/Intensity of Each Focus when Multiple Persistent Abnormal Foci of Activity were Present on MIBI-SPECT/RPJ Studies

Scintigraphic findings	Total	True positive	False positive
Single focus	45 (44)*	44 (43)	1 (1)
Multiple Foci			
No. 1 focus	13 (8)	11 (6)	2 (2)
No. 2 focus	13 (8)	6 (2)	7 (6)
No. 3 focus	5 (0)	4 (0)	1 (0)
No. 4 focus	3 (0)	2 (0)	1 (0)
Total	34 (16)	23 (8)	11 (8)

*The numbers outside parenthesis indicate data from the entire population; inside parenthesis are data from patients with primary hyperparathyroidism.

MIBI-SPECT/RPJ abnormal focus was identified and excised. QPTH information was exceptionally useful in another 5 patients with false-positive or false-negative scintigraphic lesions, and in one additional patient with two abnormal glands. In these 6 patients, QPTH showed persistently high levels and prompted continuing exploration until the single or the second abnormal gland was found and excised. Finally, in the two patients with middle/lower mediastinal abnormal glands, QPTH levels did not change at the conclusion of the cervical exploration because the abnormal tissue was not excised, and the patients remained hypercalcemic.

DISCUSSION

The tomographic imaging approach and the criteria for interpretation followed in this study resulted in identification and accurate localization of all but two (51 of 53) of the primary adenomas and all but two (16 of 18) of the hyperplastic and MEN glands with an overall sensitivity of 94% (Table 1). The data indicated that the test had a high sensitivity and specificity for localizing abnormal parathyroid glands and that it was clinically useful because it helped to improve the efficiency of parathyroidectomy.

Due consideration was given to the possibility of improving the sensitivity of the test. The four abnormal parathyroid glands, which were missed by scintigraphy, were not by any means the smallest lesions in this series. It was noticed that the second set of images of the false-negative studies might have been more than optimally delayed, as they were acquired between 3½ and 5½ hr after injection, but one third of the true-positive studies were acquired equally late. A review of the images indicated that at least two lesions not seen on delayed studies were present on early images. It may be concluded that discharge of MIBI from the parathyroid lesions is variable and that imaging at an earlier time might have been more successful in localizing the abnormalities missed. Therefore, delayed imaging may better be performed at an optimal time, which appears to be between 2 and 3 hr, although exceptional lesions may discharge MIBI even earlier.

MIBI-SPECT/RPJ had a clinically acceptable specificity of 92–98% (Table 1). When considering the number of abnormal foci visualized per study, all but one of the 45 single foci were true positive (Table 3). When more than one focus was present on scintigraphy the most intense lesion (no. 1) was true positive in the majority of the patients, whereas the second most intense lesion (no. 2) was more often false positive. Therefore, it is evident that in primary hyperparathyroidism, the single or the most intense focus represents the abnormal parathyroid gland (with a sensitivity of 92% and a specificity of 98% in this group of patients), and should be identified and excised first. This approach will cure the majority of patients, but it does not guarantee complete excision of all abnormal tissue in all patients. Indeed, even if the second most intense (no. 2) focus was to be excised as well, the sensitivity for the primary abnormalities would have risen to 96% (at the expense of specificity which would have decreased to 94%). Although seemingly excellent, these figures allow for 4–8% surgical failures and an unspecified increase in the operative time, if the operation is based solely on scintigraphy. This is the area in which QPTH measurements have made the greatest impact.

QPTH measurements not only helped shorten the operative time by confirming the excision of abnormal parathyroids in cases with true-positive scintigraphy, but they also made higher cure rate possible by guiding the surgeon to pursue and excise the second most intense lesion when parathormone levels did not fall after the excision of the single or most intense lesion. Finally, QPTH measurements were particularly helpful in two patients with false-negative SPECT studies. One of these patients had two adenomas, but only one was visualized. For these patients, the surgeon had to search, find and excise the undetected single or second abnormal parathyroid.

The combined application of preoperative MIBI-SPECT/RPJ and the intraoperative QPTH measurements had a significant impact on the success and speed of parathyroidectomy in primary hyperparathyroidism as compared to previous records, when the performance of an experienced surgeon was evaluated. Admittedly, there were two patients with middle/lower mediastinal lesions who could not be cured by neck exploration but the value of the MIBI-SPECT/RPJ to correctly and precisely localize the abnormality in the mediastinum was not appreciated at that time. Neither was it known that combined imaging with skeletal and blood pool agents would provide greater accuracy in localization. With the current experience a transthoracic approach would be followed at the outset in these cases. Both these patients had a meticulous cervical exploration and in each patient three normal parathyroid glands were found. In addition, both had high levels of intact PTH measured by radioassay, specific for parathyroid lesions. This assay does not detect the PTH-associated hormone (protein) which is secreted by lung tumors (*25*). Scintigraphy showed the ectopic abnormal parathyroid glands in the mediastinum (Fig. 4). Based on all of the above data which is sufficiently convincing, the diagnosis was made without histological confirmation and these two patients were retained in this analysis.

Three-dimensional localization of the parathyroid abnormalities guided the surgeon to decide not only the side (R/L) and the axial level of the surgical approach, but also the depth from the anterior frontal plane where the lesion was located. This helped to reduce the time required to reach and remove the abnormality. Decrease in operation room time was both clinically and financially advantageous. Planar images were 10% less sensitive than MIBI-SPECT/RPJ in visualizing the abnormal parathyroids ($p < 0.1$) and could not provide in-depth information.

The SPECT/RPJ approach had as high a sensitivity and specificity as reported for the dual-radioisotope (subtraction) approach (*26*) and together with the accurate in-depth information appeared to have the potential to eliminate the need to use additional imaging modalities (CT or MRI) recommended by other investigators (*16*).

MIBI-SPECT/RPJ was found successful in visualizing abnormal glands in patients with secondary parathyroid hyperplasia and MEN hyperparathyroidism, but the number of patients studied was small. In addition, in hyperplasia, the usual surgical practice is to find all 4 parathyroid glands and remove 3 to 3½ of them. Imaging is helpful, particularly for localizing ectopic glands, which are unusual. Whether imaging should be performed in all cases of secondary hyperparathyroidism, or only in patients in whom not all glands could be found at surgery, needs to be determined. There is a need for preoperatively localizing abnormal glands in MEN and further experience with MIBI-SPECT/RPJ appears to be warranted.

Finally, in patients with other tumors visualized by MIBI, the application of additional scintigraphy with other tumor imaging agents, such as ^{67}Ga (Fig. 5), may enhance the usefulness of the test.

CONCLUSION

In primary hyperparathyroidism, the combined use of preoperative imaging with MIBI-SPECT/RPJ and intraoperative measurements of PTH by QPTH assay improved the success rate of parathyroidectomy and dramatically shortened the operative time. The results indicated that this was a cost-effective and clinically useful approach. Additional scintigraphy with skeletal, blood pool and malignant tumor imaging agents occasionally enhanced the usefulness of this method.

ACKNOWLEDGMENTS

Presented in part at the 150th meeting of the Southern Surgical Association, Hot Springs, VA, December 5–8, 1993, and at the 41st annual meeting of the Society of Nuclear Medicine, Orlando, FL, June 5–8, 1994.

REFERENCES

1. Goris ML, Basso LV, Keeling C. Parathyroid imaging. *J Nucl Med* 1984;32:887–889.
2. Consensus Development Conference Panel. Diagnosis and management of a symptomatic primary hyperparathyroidism: consensus development conference statement. *Ann Intern Med* 1991;114:593–597.
3. Coakley AJ. Parathyroid imaging—how and when. *Eur J Nucl Med* 1991;18:151–152.
4. Ferlin G, Borsatso N, Perelli R. New perspectives in localizing enlarged parathyroids by technetium-thallium subtraction scan. *J Nucl Med* 1983;24:438–441.
5. Young AE, Gaunt JL, Croft DN, et al. Location of parathyroid adenomas by thallium-201 and technetium-99m subtraction scanning. *Br Med J* 1983;286:1384–1386.
6. Corcoran MO, Seifacian MA, George SL, Milroy SE. Localization of parathyroid adenomas by thallium-201 and technetium-99m subtraction scanning. *Br Med J* 1983;286:1751–1752.
7. Miller DL, Doppman JL, Shawker TH, et al. Localization of parathyroid adenomas in patients who have undergone surgery. 1. Noninvasive imaging methods. *Radiology* 1987;136:133–137.
8. MacFarlane SD, Hanelin LG, Taft DA, Ryan JA Jr, Fredlund PN. Localization of abnormal parathyroid glands using thallium-201. *Am J Surg* 1984;148:7–12.
9. Okerlund MD, Sheldon K, Corpuz S, et al. A new method with high sensitivity and specificity for localization of abnormal parathyroid glands. *Ann Surg* 1984;200:381–388.
10. Sandrock D, Merino MJ, Norton JA, Neumann RD. Parathyroid imaging by Tc/Tl scintigraphy. *Eur J Nucl Med* 1990;16:607–613.
11. Gimlette TMD, Brownless MS, Taylor WH, Shields R, Simkin EP. Limits to parathyroid imaging with thallium-201 confirmed by tissue uptake and phantom studies. *J Nucl Med* 1986;27:1262–1265.
12. Fogelman I, McKillop JH, Bessent RG, et al. Successful localization of parathyroid adenomata by thallium-201 and technetium-99m subtraction scintigraphy: description of an improved technique. *Eur J Nucl Med* 1984;9:545–547.
13. Coakley AJ, Kettle AG, Wells CP, O'Doherty MJ, Collins RE. Technetium-99m-sestamibi: a new agent for parathyroid imaging. *Nucl Med Commun* 1989;10:791–794.
14. O'Doherty MJ, Kettle AG, Wells P, Collins REC, Coakley AJ. Parathyroid imaging with technetium-99m-sestamibi: preoperative localization and tissue uptake studies. *J Nucl Med* 1992;33:313–318.
15. Taillefer R, Boucher Y, Potvin C, Lambert R. Detection and localization of parathyroid adenomas in patients with hyperparathyroidism using a single radionuclide imaging procedure with technetium-99m-sestamibi (double phase study). *J Nucl Med* 1992;33:1801–1807.
16. Numerow LM, Morita ET, Clark OH, et al. Prospective comparison of Tc-99m-sestamibi scintigraphy, MR imaging and sonographic techniques for preoperative hyperparathyroidism. *Radiology* 1994;193P:269.
17. Irvin GL, Dembrow VD, Prudhomme DL. Operative monitoring of parathyroid gland hyperfunction. *Am J Surg* 1991;162:299–302.
18. Irvin GL, Dembrow VD, Prudhomme DL. Clinical usefulness of an intraoperative "quick PTH" assay. *Surgery* 1993;114:1019–1023.
19. Brown RC, Aston JP, Weeks I, Woodhead JS. Circulating intact parathyroid hormone measured by a two-site immunochemiluminometric assay. *J Clin Endocrinol Metab* 1987;65:407–414.
20. Hage DS, Kao PC. High-performance immunoaffinity chromatography and chemiluminescent detection in the automation of a parathyroid hormone sandwich immunoassay. *Anal Chem* 1991;63:586–595.
21. Irvin GL III, Deriso GT. A new, practical intraoperative parathyroid hormone assay. *Am J Surg* 1994;168:466–468.
22. Irvin GL III, Prudhomme DL, Deriso GT, Sfakianakis GN, Chandarlapaty SKC. A new approach to parathyroidectomy. *Ann Surg* 1994;219:574–581.
23. Sfakianakis GN, Foss J, Georgiou M, Irvin GL III, et al. The role of preoperative SPECT-99m-sestamibi imaging and intraoperative PTH measurement in parathyroidectomy. *J Nucl Med* 1994;35:68P.
24. Talton DA, Goldwasser SM, Reynolds RA, Walsh ES. Volume rendering algorithms for the presentation of 3-D medical data. *Proceedings Volume III: NCGA computer graphics 8th annual conference*. 1987:11.
25. Nussbaum SR, Potts JT Jr. Immunoassays for parathyroid hormone in the diagnosis of hyperparathyroidism. *J Bone Min Res* 1991;6:1–84.
26. Neuman DR, Esselstyn CB Jr, Go RT, et al. Comparison of double-phase Tc-99m-sestamibi SPECT with simultaneous I-123, Tc-99m-sestamibi subtraction SPECT for preoperative localization of parathyroid tissue. *Radiology* 1994;193P:246.